

Tailoring the magnetic anisotropy in CoRh nanoalloys

M. Muñoz-Navia,¹ J. Dorantes-Dávila,^{1,a)} D. Zitoun,² C. Amiens,² N. Jaouen,³ A. Rogalev,³ M. Respaud,⁴ and G. M. Pastor⁵

¹Instituto de Física, Universidad Autónoma de San Luis Potosí, 78000 San Luis Potosí, Mexico

²Laboratoire de Chimie de Coordination, CNRS, F-31077 Toulouse, France

³European Synchrotron Radiation Facility, 6 rue Jules Horowitz, 38043 Grenoble, France

⁴LPCNO, INSA, Université de Toulouse, 135 avenue de Rangueil, F-31077 Toulouse, France

⁵Institut für Theoretische Physik, Universität Kassel, 34132 Kassel, Germany

(Received 5 September 2009; accepted 16 November 2009; published online 7 December 2009)

CoRh alloy nanoparticles (NPs) show nontrivial correlations between chemical and magnetic order that lead to a remarkable nonmonotonous dependence of the magnetic anisotropy energy as a function of composition. Combining experiment and theory we demonstrate how the induced $4d$ moments and the $3d$ – $4d$ interfaces control the magnetoanisotropic behavior. New possibilities of tailoring the magnetic characteristics of NPs are thus opened. © 2009 American Institute of Physics. [doi:10.1063/1.3272000]

Nanoalloys are emerging as an important multidisciplinary field with increasing impact throughout nanoscience and technology.^{1–3} Magnetic phenomena are particularly interesting in view of controlling and optimizing the spin and orbital moments, magnetic order, and magnetic anisotropy energy (MAE) by varying the composition and distribution of the elements within the nanoparticles (NPs). These are very important issues, especially for applications, since the MAE determines the magnetization direction as well as its stability. It is therefore quite remarkable that very little is still known about the microscopic origin of the MAE in nanoalloys and about the possibilities of systematic material optimization that it offers.^{3,4} Previous experimental studies in CoRh NPs have demonstrated the concentration dependence of the average magnetic moments,² while theory has revealed interesting changes in the MAE for small sizes ($N < 100$ atoms).⁵ It is the purpose of this letter to combine experiment and theory to determine the MAE of CoRh NPs as a function of concentration in order to understand its microscopic origin as an important step toward magnetic nanoalloy design.

The NPs have been synthesized in solution by decomposition of organometallic precursors in the presence of a stabilizing polyvinylpyrrolidone polymer as described in Ref. 2. For the present study samples with Co concentration $x = 0.76, 0.49,$ and $0.25,$ and particle diameter ϕ in the range $1.6 \leq \phi \leq 2.5$ nm were synthesized. The wide angle x-ray scattering patterns of $\text{Co}_{0.49}\text{Rh}_{0.51}$ and $\text{Co}_{0.76}\text{Rh}_{0.24}$ NPs are well fitted with a compact structure having a nearest neighbor (NN) distance $d_{\text{NN}} \approx 0.269$ and 0.263 nm, respectively.⁶ The $\text{Co}_{0.25}\text{Rh}_{0.75}$ NPs show a bulklike fcc structure with $d_{\text{NN}} \approx 0.269$ nm. The contrast observed in high-resolution transmission-electron microscopy on larger isolated particles indicates that the NPs are all bimetallic with close-packed structures having most probably a Rh-rich inner core and a Co-rich outer shell.

Tailoring the NP magnetic properties involves a number of serious challenges. Different growth conditions can lead to segregated clusters with either a $4d$ core and a $3d$ outer shell or vice versa. Postsynthesis manipulations can induce different degrees of intermixing at the $3d/4d$ interfaces in-

cluding surface diffusion, ordered or disordered alloys, etc. Controlling the distribution of the elements within alloy clusters is therefore a crucial issue. In order to quantify the role of chemical order in magnetic nanoalloys we perform a comprehensive set of electronic calculations for clusters having $N \approx 500$ atoms, Co concentrations $x \approx 0.25, 0.5,$ and $0.75,$ and different distributions of the Co and Rh atoms. The theory is based on a realistic *spd*-band tight-binding Hamiltonian describing the redistributions of the spin- and orbital-polarized density (SOPD), as well as the spin-orbit (SO) interactions H_{SO} at the origin of magnetic anisotropy at the same electronic level.^{5,7} Accurate self-consistent calculations are performed for each orientation δ of the spin magnetization \vec{S} . The MAE $\Delta E_{\delta\gamma} = E_{\delta} - E_{\gamma}$ is derived in a nonperturbative way as the difference between the electronic energies E_{δ} . This is particularly important for weak ferromagnetic systems, such as Rh-based alloy clusters, where rotating \vec{S} results in significant changes in the SOPD. Besides effectiveness, our model approach provides a conceptually attractive alternative to density functional methods, since it reveals the important correlations between chemical order and magnetic behavior in a straightforward and transparent way. These features will be exploited systematically in the following.^{5,7}

In Fig. 1 theoretical results are given for the magnetiza-

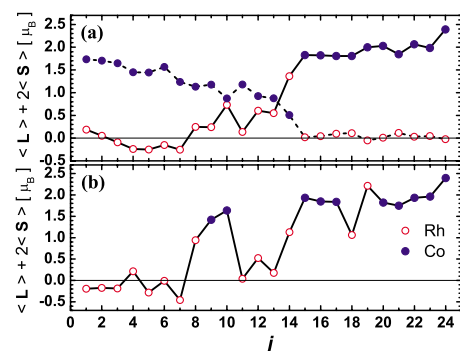


FIG. 1. (Color online) Local magnetic moments along the easy axis of 2 nm $\text{Co}_{0.5}\text{Rh}_{0.5}$ clusters ($N = 489$ atoms). j labels the nonequivalent atomic sites ordered by increasing distance to the central atom. (a) Fully segregated Co core with Rh shells (dashed) and Rh core with Co shells (solid). (b) Rh core with Co outer shells and intermixing at the interface.

^{a)}Electronic mail: jdd@ifisica.uaslp.mx.

tion profile of 2 nm octahedral fcc-like $\text{Co}_{0.5}\text{Rh}_{0.5}$ NPs with three different chemical orders ($N=489$ atoms). These are representative of a much larger number of studied structures, shapes, sizes, and compositions. In the case of a fully segregated Co core with a Rh outer shell [dashed in Fig. 1(a)] the Co magnetic moments at the innermost atoms are similar to the Co bulk moment and decrease as one goes from the center to the CoRh interface. Only very small magnetic moments are induced at the Rh, which show weak oscillations as we move away from the interface toward the surface (larger j in Fig. 1). The significant reduction in the Co moments at the interface is not compensated by the tiny induced Rh moments. Consequently, the calculated average moment per CoRh unit $\bar{\mu}_{\text{CoRh}}=1.30\mu_{\text{B}}$ (spin moment $\mu_{\text{S}}=1.21\mu_{\text{B}}$ and orbital moment $\mu_{\text{L}}=0.09\mu_{\text{B}}$) remains fairly small, actually smaller than in pure Co clusters or surfaces.

The situation changes qualitatively if one considers a Rh core with Co outer shells [solid in Fig. 1(a)]. Now the Co moments are largest at the surface ($19 \leq j \leq 24$) and decrease only slightly at the CoRh interface. The induced Rh moments are quite important, particularly at the interface [$\mu(j) = (0.5-1.3)\mu_{\text{B}}$ for $10 \leq j \leq 14$]. They yield, despite reductions and changes in sign at the innermost shells ($1 \leq j \leq 9$), a significant net contribution to the average moment $\bar{\mu}_{\text{CoRh}} = 2.08\mu_{\text{B}}$ ($\mu_{\text{S}}=1.75\mu_{\text{B}}$ and $\mu_{\text{L}}=0.33\mu_{\text{B}}$) which is now larger than those in bulk alloys of similar concentrations. These contrasting behaviors demonstrate the crucial role of chemical order on the magnetic properties of nanoalloys. In fact, only one of these arrangements (a Rh-core with a outer Co shells) is consistent with the measured saturated magnetization [$\bar{\mu}_{\text{CoRh}}^{\text{expt}} = (2.38 \pm 0.05)\mu_{\text{B}}$ for 2 nm $\text{Co}_{0.5}\text{Rh}_{0.5}$].²

The dependence on chemical order can be understood by contrasting the different local atomic environments. In the first case (Co core and Rh shell) all Co atoms have bulklike coordination with less Co than Rh NNs at the interface. This increases the effective local d -band width at Co atoms and reduces the local Co moments. Moreover, the interface Rh atoms have few Co NN with weakened moments, so that the induced Rh polarization is quite small. Finally, the curvature at the surface of 2 nm particles ($N \approx 500$) is not large enough to sustain the formation of local Rh moments (Rh_N is magnetic only for $N \leq 30-50$).⁸ In contrast, in the second case (Rh core and Co shell) there are several factors that *enhance* magnetism as follows: (i) The reduction in coordination number at the surface Co atoms increases the local moments, in particular, the orbital ones. (ii) The interface Co atoms, being outside, have more Co than Rh NNs, so that the d -band broadening is weaker. (iii) The Rh atoms at the interface have here a majority of strongly magnetic Co NNs, which induce important Rh moments over several interatomic distances. These trends are common to all studied compact clusters with different surface shapes and sizes ($N > 100$). Since $4d$ magnetism and the associated MAEs can only survive close to the $3d-4d$ interfaces, the shape and structure of the latter and the possible interactions with the cluster surface are crucial for the magnetic behavior of nanoalloys.

Real NPs need not have perfect interfaces with fully segregated species. We have therefore studied more complex chemical orders by considering various intermixed configurations at the interface. A representative example is shown in Fig. 1(b). This corresponds to a Rh core with Co outer shells including intermixing between atoms at CoRh interface, i.e.,

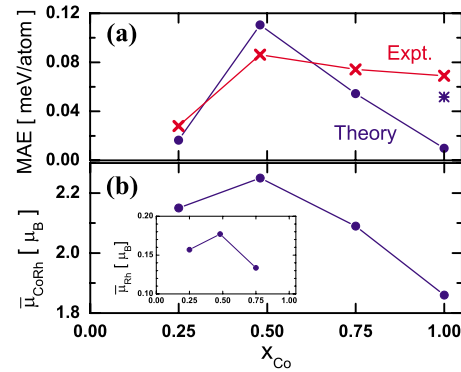


FIG. 2. (Color online) (a) Anisotropy energy and (b) average moment per CoRh unit $\bar{\mu}_{\text{CoRh}}$ of 2 nm $(\text{Co}_x\text{Rh}_{1-x})_N$ from experiment (crosses) and theory (dots, $N=489$ atoms). The star refers to a dodecahedral cluster shape ($x=1$). The inset shows the average moment $\bar{\mu}_{\text{Rh}}$ induced at the Rh atoms.

exchanging 60 atoms at the outermost Rh layer and at the innermost Co layer. For simplicity, complete sets of symmetrically equivalent atoms are interchanged [$j=9$ and 10 with $j=18$ and 19 , see Fig. 1(b)] so that the point-group symmetry of the clusters is preserved. One observes that intermixing yields an important enhancement of the spin and orbital Rh moments which have a Co-rich local environment, while the Co moments are not much affected. The net result is a significant increase in the average magnetic moment that improves the agreement with experiment ($\bar{\mu}_{\text{CoRh}}=2.24\mu_{\text{B}}$ with $\mu_{\text{S}}=1.90\mu_{\text{B}}$ and $\mu_{\text{L}}=0.34\mu_{\text{B}}$ for $N=489$ atoms). Further calculations including surface segregation and random alloy arrangements show that the precise choice of intermixing does not change the trends in the average moment or in the MAE.⁵ The enhancement of $4d$ moments due to intermixing is explained by the large spin and orbital polarizability of Rh atoms with increasing number of Co NNs, and by the robustness of the nearly saturated Co spin moments. In fact, concerning the local moments, Rh atoms surrounded mainly by Co NNs behave almost like Co atoms.

The role of $4d$ magnetic contributions has been determined experimentally by means of x-ray magnetic circular dichroism measurements at the $L_{2,3}$ Rh thresholds. These show that the Rh atoms in $\text{Co}_{0.5}\text{Rh}_{0.5}$ clusters carry significant magnetic moments. Using the usual sum rules we derive $\mu_{\text{L}}/\mu_{\text{S}}=0.066$ for the orbital to spin ratio. This is in good agreement with our theoretical results $\mu_{\text{L}}/\mu_{\text{S}}=0.076$ for 2 nm NPs having a Rh core and outer Co shells. In contrast, the calculations assuming a Co core with Rh shells yield far too small values ($\mu_{\text{L}}/\mu_{\text{S}} \leq 0.01$). Comparison between experimental and theoretical results indicates therefore that the synthesized NPs have a Rh-core with Co outer shell structure, in agreement with the information derived from independent microscopy studies.^{6,9}

Low temperature ($T=2$ K) superconducting quantum interference device measurements of the average magnetization per CoRh unit $\bar{\mu}_{\text{CoRh}}$ of 2 nm CoRh particles obtained in a $5T$ applied field show an interesting nonmonotonous concentration dependence as follows: $\bar{\mu}_{\text{CoRh}}(5T)=1.94, 2.16, 1.91, \text{ and } 0.88\mu_{\text{B}}$ for $x=1, 0.75, 0.5, \text{ and } 0.25$, respectively. Unfortunately, the lack of saturation in these results, and the fact the expected magnetization increase $\Delta\bar{\mu}$ upon saturation depends strongly on x , prevent achieving quantitative conclusions. Although a nonmonotonous x -dependence of $\bar{\mu}_{\text{CoRh}}$ is also found in the calculations reported in Fig. 2(b), some

discrepancies between theory and experiment remain. This concerns, in particular, the values for $x \approx 0.75$ which seem to be significantly underestimated. This is probably a consequence of an underestimation of the change in the Co moments upon Rh doping. In fact, *ab initio* calculations on small CoRh clusters ($N \leq 10$ atoms) yield Co moments that are about 10% larger than the predictions of our model. This can be traced back to an increase in the number of Co d holes due to Rh doping (charge transfer effect). However, we have verified, by varying the number of d electrons and the exchange integrals, that this does not affect the trends in the MAE. In fact, the MAE is dominated by the contribution of the induced Rh moments as discussed below.

In Fig. 2(a) the concentration dependence of the MAE of 2 nm CoRh NPs is shown. The experimental results were obtained by fitting the zero-field-cooled and field-cooled magnetization curves using a standard uniaxial Stoner–Wohlfarth model and a log-normal size distribution as described in Ref. 10. The theoretical results correspond to fcc-like octahedral clusters having a Rh core with a Co outer shell ($N=489$ atoms). A remarkable nonmonotonous behavior is observed. Starting from pure Co NPs ($x=1$) and increasing the Rh content, the MAE first increases, reaching a maximum around $x=0.5$ and then decreasing rapidly as x is further reduced. Experiment and theory deliver quite consistent results, except for $x=1$, where the calculations underestimate experiment by a factor of 7. This is most probably due to the high symmetry and surface compactness of the considered octahedral structure. Indeed, a large part of the discrepancy is removed by considering a dodecahedral cluster shape with a somewhat more open surface [see Fig. 2(a)]. The microscopic origin of the concentration dependence can be explained by analyzing the local moments, in particular, the induced Rh moments as a function of x . As shown in Fig. 2(b) the magnetic moment per Co atom and the average magnetic moment $\bar{\mu}_{\text{Rh}}$ at Rh atoms (inset figure) increase with increasing Rh content until the Co concentration becomes so low that the overall cluster magnetization breaks down. In fact, the higher magnetic susceptibility of the Rh clusters, as compared with Rh bulk, also explains why the

optimal Rh concentration is larger in CoRh NPs ($x_{\text{max}} \approx 0.5$ for 2 nm NPs) than in macroscopic CoRh alloys.¹¹ Moreover, in order to confirm the dominant role of the Rh contribution to the MAE, we have artificially switched off the spin-orbit coupling at the Rh atoms and found no enhancement of MAE but a decrease with increasing Rh content. The correlation between induced Rh moments and MAE is found to be a quite general trend, which reflects the microscopic mechanisms controlling the subtle magnetoanisotropic behavior of 3d–4d nanoalloys. New possibilities for tailoring the magnetic behavior of nanostructures for specific applications are thereby opened.

¹S. Sun, C. B. Murray, D. Weller, L. Folks, and A. Moser, *Science* **287**, 1989 (2000).

²D. Zitoun, M. Respaud, M.-C. Fromen, M. J. Casanove, P. Lecante, C. Amiens, and B. Chaudret, *Phys. Rev. Lett.* **89**, 037203 (2002).

³S. Yin, R. Moro, X. Xu, and W. A. de Heer, *Phys. Rev. Lett.* **98**, 113401 (2007); M. E. Gruner, G. Rollmann, P. Entel, and M. Farle, *ibid.* **100**, 087203 (2008); M. B. Knickelbein, *Phys. Rev. B* **75**, 014401 (2007); F. Tournus, A. Tamion, N. Blanc, A. Hannour, L. Bardotti, B. Prével, P. Ohresser, E. Bonet, T. Epicier, and V. Dupuis, *Phys. Rev. Lett.* **77**, 144411 (2008).

⁴P. Gambardella, S. Rusponi, M. Veronese, S. S. Dhesi, C. Grazioli, A. Dallmeyer, I. Cabria, R. Zeller, P. H. Dederichs, K. Kern, C. Carbone, and H. Brune, *Science* **300**, 1130 (2003).

⁵M. Muñoz-Navia, J. Dorantes-Dávila, D. Zitoun, C. Amiens, B. Chaudret, M.-J. Casanove, P. Lecante, N. Jaouen, A. Rogalev, M. Respaud, and G. M. Pastor, *Faraday Discuss.* **138**, 181 (2008).

⁶M. C. Fromen, J. Morillo, M.-J. Casanove, and P. Lecante, *Europhys. Lett.* **73**, 885 (2006).

⁷G. M. Pastor, J. Dorantes-Dávila, S. Pick, and H. Dreyssé, *Phys. Rev. Lett.* **75**, 326 (1995); G. Nicolas, J. Dorantes-Dávila, and G. M. Pastor, *Phys. Rev. B* **74**, 014415 (2006).

⁸A. J. Cox, J. G. Louderback, S. E. Apsel, and L. A. Bloomfield, *Phys. Rev. B* **49**, 12295 (1994).

⁹E. O. Berlanga-Ramírez, F. Aguilera-Granja, J. M. Montejano-Carrizales, A. Díaz-Ortiz, K. Michaelian, and A. Vega, *Phys. Rev. B* **70**, 014410 (2004).

¹⁰M. Respaud, J. M. Broto, H. Rakoto, A. R. Fert, L. Thomas, B. Barbara, M. Verelst, E. Snoeck, P. Lecante, A. Mosset, J. Osuna, T. Ould Ely, C. Amiens, and B. Chaudret, *Phys. Rev. B* **57**, 2925 (1998).

¹¹G. R. Harp, S. S. P. Parkin, W. L. O'Brien, and B. P. Tonner, *Phys. Rev. B* **51**, 12037 (1995).